PHYSICAL REVIEW B VOLUME 38, NUMBER 12 15 OCTOBER 1988-II

# Microcrystalline and interface structure of metallic multilayers from x-ray spectra

Mary Beth Stearns
*Department of Physics, Arizona State University, Tempe, Arizona 85287*
(Received 13 January 1988)

A calculation of the large-angle x-ray-scattering spectra is derived for crystalline multilayered films having extended interfaces with linear random alloy-composition variation. The model also includes the presence of crystallites of the pure components. By fitting the calculated and measured spectra the structural parameters such as the individual layer thicknesses, bilayer and interface thicknesses, and lattice spacings, as well as coherence length of the multilayer and crystallite sizes in the direction of growth of the multilayer, can be determined. In the fitting procedure these parameters are essentially independent and can be determined to within fractions of an angstrom. A comparison of the calculated and measured spectra for several Co/Cr multilayers is made and briefly discussed.

## I. INTRODUCTION

X-ray diffraction is one of the most widely used techniques for characterizing the structure of multilayered films. Numerous models have appeared in the literature[1,2] which emphasize various features of the superlattices. We have developed two models for large-angle $\theta-2\theta$ scattering which realistically treat the most salient features of typical metallic multilayered structures. They are especially applicable to metallic multilayers (ML) where the atomic sizes of the two metals are moderately mismatched. The models represent the ML as having pure regions of materials $A$ and $B$ separated by interfacial regions. Two specific models are considered one where the variation in lattice constant in the interface is represented by two steps and the other where the lattice constant varies linearly, as expected for random alloy-compositional mixing across the interfaces. It has been observed that multilayers with one of the components having the hcp structure often contain crystallites of other hcp orientations than that which grows in the multilayer.[3,4] This occurs because the [10.0], [00.2], and [10.1] hcp orientations have very similar in-plane areas per atom. For multilayer combinations having moderately mismatched $d$ spacings or atomic sizes the binding energy between the layers is maximized by selecting the crystal-growth orientations of the two components which have the closest in-plane areas per atom. For Co/Cr multilayers the bcc structure of the Cr has by far the smallest in-plane area per atom in the (110) planes so the Cr layers grow in the [110] direction. This causes the Co layers to grow in the [10.1] hcp orientation since its in-plane area per atom is nearly the same as that of (110) Cr. However as the layers get thicker the other hcp orientations having similar in-plane areas are also found to be present in the ML films. So the models presented here also include such crystallites. In practice all the structural parameters such as the lattice spacings, individual layer thicknesses, bilayer and interfacial thicknesses, as well as coherence length of the ML and crystallite sizes in the direction of growth, have been obtained for the Co/Cr ML system by fitting with these models.

A derivation of the models is presented in Sec. II. A comparison of the calculated and measured data for a few Co/Cr ML is given in Sec. III.

## II. CALCULATION OF THE SCATTERING INTENSITIES

### A. Model I

For model I one-half of the interface atoms are assumed to be pure atoms $A$ with lattice spacing of $d_A+\delta$ and one-half are pure atoms $B$ with spacing $d_B-\delta$. Where $\delta=(d_B-d_A)/(N+1)$. The advantage of this model is that all regions of the ML can be represented by the functional form $\sin^2(Nx)/\sin^2 x$. Since the intensities are calculated using a computer this is of no real advantage, but it is of interest to use this rather unrealistic model in order to see how it differs from the more realistic model II. It was found that reasonably good fits to the measured spectra could be made with this model but it required interfacial thicknesses that were unreasonably large. For a few of the Co/Cr ML even assuming that they were all interface did not reduce the satellite heights sufficiently to give good fits. Another feature of the Co/Cr spectra that could not be obtained with this model was the observed difference in spacing from the main peak of the upper and lower satellites for equal layer thickness ML. In the Co/Cr spectra the lower satellite is generally closer to the main peak than the upper satellites. Model I always produced equal spacing of the satellites for equal layer thickness ML. Since the fits obtained with model II were much more satisfactory than those with model I, it will not be discussed further.

### B. Model II

The basic assumption behind model II is that the interfaces are assumed to be completely miscible random alloys having a linear compositional variation. The layer spacings resulting from such assumptions are shown

 ©1988 The American Physical Society

schematically in Fig. 1 which shows the $d$-spacing variation with layer number; it is similar to the composition variation. Thus the ML is composed of $N_A$ and $N_B$ atomic layers of the pure materials $A$ and $B$ having $d$ spacings $d_A$ and $d_B$, respectively. The front interface between pure regions of atoms $A$ and $B$ contains $N_F$ atomic layers with $d$ spacings in the $n$th layer, starting from the pure $A$ region, vary linearly as given by

$$d_n^F = d_A + n\varepsilon_F , \tag{1}$$

where $\varepsilon_F = (d_B - d_A)/(N_F+1)$. Similarly the rear interface contains $N_R$ atomic layers whose $d$ spacing in the $n$th layer from the pure $B$ region vary as

$$d_n^R = d_B - n\varepsilon_R , \tag{2}$$

where $\varepsilon_R = (d_B - d_A)/(N_R+1)$.

Various expressions for the scattering from crystallites are discussed in many books on x-ray scattering.[5,6] We closely follow these derivations. As shown in Fig. 1 there are four regions to consider: the front interface, pure material $B$, the rear interface, and pure material $A$. The growth direction of the ML is taken as the $z$ direction. The amplitudes for scattering an x ray through an angle $2\theta$ with the scattering vector in the $z$ direction from a crystallite of the ML are given by the following.

Front interface:

$$\mathcal{A}_F \propto S \sum_{n=1}^{N_F+1} \rho_n^F f_n^F D_n^F \times \exp\{i\phi[nd_A + \varepsilon_f n(n+1)/2]\} , \tag{3}$$

where $\rho_n$ is the area density per atom in the $n$th plane of the front interface of the ML, and $f_n$ and $D_n$ are similarly the atomic scattering factors and Debye-Waller factors, respectively. In the $n$th plane of the front interface $f_n^F = f_A + (f_B - f_A)n/(N_F+1)$ where $f_A$ and $f_B$ are the atomic scattering factors of the atoms $A$ and $B$, respectively. $D_n^F$ and $\rho_n^F$ are similarly defined. The quantity $\phi = 4\pi \sin\theta/\lambda_x$ where $\lambda_x$ is the x-ray wavelength and $S = N_x^A N_y^A/\rho_A$ or $N_x^B N_y^B/\rho_B$ is the in-plane area of the ML crystallite.

Pure material $B$:

$$\mathcal{A}_B \propto S\rho_B f_B D_B \exp[i\phi(x_1 + N_B d_B/2)] \times \sin[(N_B-1)\phi d_B/2]/\sin(\phi d_B/2) , \tag{4}$$

where $x_1 = N_F\bar{d} + d_B$ and $\bar{d} = (d_B + d_A)/2$. All other quantities are defined in analogy to the front-interface region.

Rear interface:

$$\mathcal{A}_R \propto S \exp(i\phi x_2) \sum_{n=1}^{N_R+1} \rho_n^R f_n^R D_n^R \times \exp\{i\phi[nd_B - \varepsilon_R n(n+1)/2]\} , \tag{5}$$

where $x_2 = x_1 + (N_B - 1)d_B$ and $f_n^R = f_B - (f_B - f_A)n/(N_R+1)$ with $\rho_n^R$ and $D_n^R$ defined similarly.

Pure material $A$:

$$\mathcal{A}_A \propto S\rho_A f_A d_A \exp[i\phi(x_3 + N_A d_A/2)] \times \sin[(N_A-1)\phi d_A/2]/\sin(\phi d_A/2) , \tag{6}$$

where $x_3 = x_2 + N_R\bar{d} + d_A$.

The scattering amplitude for $M$ bilayers of the ML is then given by

$$\mathcal{A}_M = (\mathcal{A}_F + \mathcal{A}_B + \mathcal{A}_R + \mathcal{A}_A)\exp[i(M-1)\phi\Lambda/2] \times \sin(M\phi\Lambda/2)/\sin(\phi\Lambda/2) , \tag{7}$$

where $\Lambda$ is the bilayer thickness, $\Lambda = (N_F + N_R)\bar{d} + N_B d_B + N_A d_A$. The crystallites in the direction of growth of the ML are of the order of 120–200 Å so they are small enough to give rise to observable linewidths. The spectra were measured with Cr $K\alpha$ x rays having a longitudinal coherence of $\sim 1$ µm and a lateral coherence of $\sim 1000$ Å. Thus the intensity of scattering from a crystallite of the ML calculated from Eq. (7) is an observable quantity[5] and is given by

$$I_M(\theta) \propto P(\theta) |\mathcal{A}_M|^2 , \tag{8}$$

where $P(\theta) = [1+\cos^2(2\theta)]/2\sin\theta$; the polarization factor with a $\sin\theta$ in the denominator due to the variation with angle of the volume of the ML intercepted by the incident x-ray beam. Typically our ML are $\sim 3000$ Å thick, so absorption is negligible. In general the in-plane area of the ML is unknown so that the quantity that is calculable is

$$I_M^c = I_M(\theta)/S^2 . \tag{9}$$

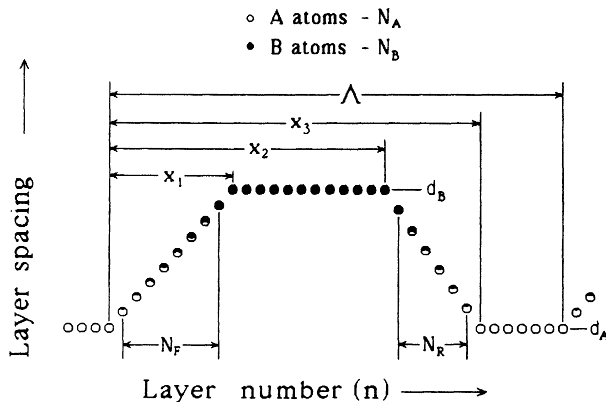


FIG. 1. Schematic diagram of variation of $d$ spacing with layer number for the trapezoidal model of a multilayered structure. Scattering from the four regions of the multilayered films is discussed in the text.

### C. Small crystallites of other pure orientations

As mentioned previously, it has been observed[3,4] that the $\theta$–$2\theta$ spectra of Co/Cr ML often contain peaks at the positions corresponding to pure [00.2] hcp Co and/or [110] Cr (these are so close in $d$ spacing as to be indistinguishable) and [10.0] hcp Co. Denoting these pure crystallites by the subscripts 1 and 2 we have, in analogy to

Eq. (4), that the intensity due to crystallites of type 1 is given by

$$I_1(\theta) \propto P(\theta) \mid A_1 \rho_1 f_1 D_1 \exp[i\phi(N_1-1)d_1] \times \sin(N_1 \phi d_1/2)/\sin(\phi d_1/2) \mid^2 , \quad (10)$$

where $N_1$ is the number of atomic planes in the direction of growth of crystallites of type 1, $d_1$ is the $d$ spacing, $A_1$ is the in-plane area, and all other quantities are similar to those defined above. Again, in general, the in-plane area is unknown and we calculate $I_1^c = I_1(\theta)/A_1^2$. Similar expressions describe the intensity due to crystallites of type 2.

### D. ML coherence length

Before summing the spectra of all the crystallites they are each broadened for the instrumental resolution assuming a Lorentzian shape. The instrumental resolution is 0.15° for the Rigaku D/Max-III spectrometer on which the spectra were taken. A further correction is necessary for the ML when the bilayer thickness is an appreciable fraction of the total ML thickness; as occurs when the number of bilayers $M$ in an ML crystallite is small. Under these conditions the ML usually has a fractional number of bilayers. This correction can be made by adding an additional broadening $\Gamma$ to the ML crystallites only. The Scherrer equations[5] is then used to obtain the fractional layer thickness corresponding to this additional broadening. Thus the corrected ML coherence length $L_M$ is given by

$$L_M = M\Lambda/(1+M\Lambda\Gamma\cos\theta/\lambda_x) \quad (11)$$

with $\Gamma$ in radians and $\cos\theta$ approximated by $[1-(\lambda_x/2\bar{d})^2]^{1/2}$. We have assumed Lorentzian shapes for the convolution of the linewidths and just added the linewidths.

### E. Total scattering intensity

Since the crystallites of ML and the pure materials scatter independently the total scattering intensity is given by

$$I_T(\theta) \propto \eta_M S^2 I_M^c + \eta_1 A_1^2 I_1^c + \eta_2 A_2^2 I_2^c , \quad (12)$$

where $\eta_M$, $\eta_1$, and $\eta_2$ are the number of the individual crystallites respectively of the ML and the two types of pure crystallites in a unit volume. Since we are only concerned with the shape of the spectra we can write Eq. (12) with only two unknown parameters as

$$I_T(\theta) \propto I_M^c + \mathscr{f}_1 I_1^c + \mathscr{f}_2 I_2^c , \quad (13)$$

where $\mathscr{f}_1 = \eta_1 A_1^2/\eta_M S^2$ and $\mathscr{f}_2 = \eta_2 A_2^2/\eta_M S^2$. The $\mathscr{f}$ values are uniquely determined by fitting the calculated and measured spectra.

### F. Average volume fractions

If the in-plane areas are known the $\mathscr{f}$ values can be used to obtain the average volume fractions of each type crystallite in the oriented crystallite volume. The in-plane areas can be obtained by measuring the x-ray scattering with the scattering wave vector near the plane of the film. As yet we have not performed these measurements since the in-plane scattering is very weak due to the random crystallite orientation in the plane of the films and should optimumly be measured using synchrotron x rays. Such measurements are being planned. Meanwhile the volume fractions can be estimated under particular assumptions about the shapes of the crystallites. There are two simple cases where these volume fractions can be evaluated.

*Case* (a). One case is that in which all the in-plane areas are the same i.e., $S = A_1 = A_2$. Here $\mathscr{f}_1 = \eta_1/\eta_M$ and $\mathscr{f}_2 = \eta_2/\eta_M$. In this case the ratio of the volumes of type 1 to ML crystallites is $\eta_1 L_1/\eta_M L_M$ where $L_1 = N_1 d_1$; similarly for type 2. Letting $g_a = 1 + \mathscr{f}_1 L_1/L_M + \mathscr{f}_2 L_2/L_M$, the volume fractions $v$ are then given by

$$v_M = 1/g_a, \quad v_{1a} = \mathscr{f}_1 L_1/g_a L_M, \quad v_{2a} = \mathscr{f}_2 L_2/g_a L_M . \quad (14)$$

*Case* (b). This case is for the crystallites which are the same size in all directions: $S = L_M^2$, $A_1 = L_1^2$, and $A_2 = L_2^2$. Here $\mathscr{f}_1 = \eta_1 L_1^4/\eta_M L_M^4$ and $\mathscr{f}_2 = \eta_2 L_2^4/\eta_M L_M^4$. Letting $g_b = 1 + \mathscr{f}_1 L_M/L_1 + \mathscr{f}_2 L_M/L_2$ for this case the volume fractions are given by

$$v_M = 1/g_b, \quad v_{1b} = \mathscr{f}_1 L_m/g_b L_1, \quad v_{2b} = \mathscr{f}_2 L_m/g_b L_2 . \quad (15)$$

A more general version of this case is that in which the shape of the ML crystallites is not assumed. Here $g = 1 + \mathscr{f}_1 S/L_1 L_M + f_2 S/L_2 L_M$ and the volume fractions are given by

$$v_M = 1/g, \quad v_1 = \mathscr{f}_1 S/g L_1 L_M, \quad v_2 = \mathscr{f}_2 S/g L_2 L_M . \quad (16)$$

Since the $\mathscr{f}$ values and $L_M$, $L_1$, $L_2$ are determined in the fitting procedure the volume fractions can be evaluated for the two above-mentioned cases.

## III. COMPARISON WITH SOME TYPICAL Co/Cr SPECTRA

Figure 2 shows some typical $\theta$–$2\theta$ spectra of several Co/Cr multilayers. Before outlining the fitting procedure we list the salient features of a spectrum and the parameters which mainly affect each feature. (1) The position of the central peak is sensitive to the relative number of layers of materials $A$ and $B$. (2) The angular difference between the first upper and lower satellites depends on the bilayer thickness $\Lambda$. These satellites are usually not spaced symmetrically with respect to the main peak; even for equal layer thicknesses. This behavior is reproduced in the trapezoidal model II. (3) The heights of the satellites relative to the main peak are sensitive to the number of interfacial layers, $N_F$ and $N_R$. (4) The widths of the peaks are determined by the number of atomic layers in the direction of growth of the crystallites, $N_A$, $N_B$, $N_1$, and $N_2$.

We emphasize that although there are a large number of parameters in the calculation they can be fit one at a time with essentially no dependence between their values. Thus the average values for all the parameters in the

direction of growth can be determined by fitting the calculated spectra to the measured spectra. We note that the calculation assumes that only the scattering within a ML crystallite is coherent and that each individual crystallite scatters independently. That this is a good assumption is confirmed by cross-sectional high-resolution transmission-electron-microscope images of these multilayers[4] which show that the layers are quite rough.

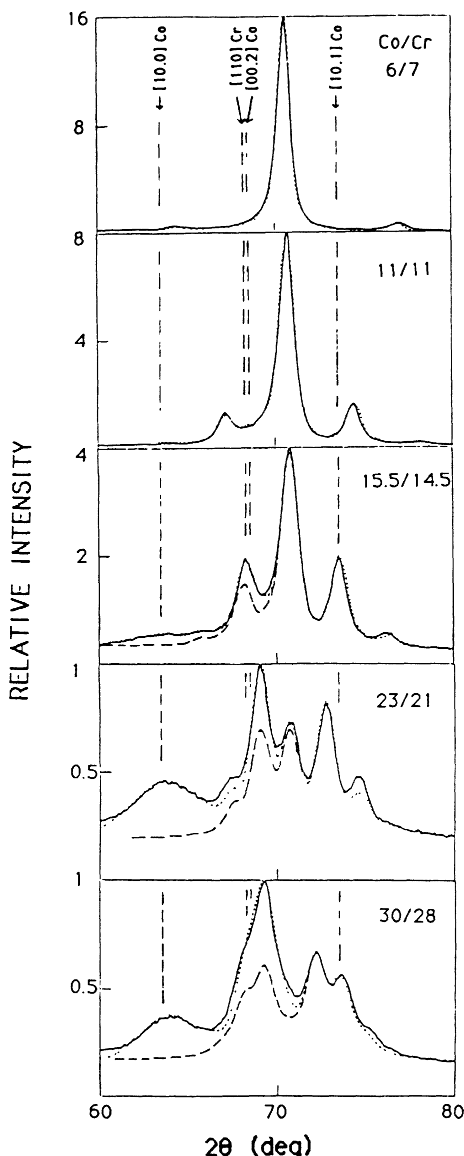


FIG. 2. Measured Cr $K\alpha$ x-ray scattering spectra of several nearly equal layer thickness Co/Cr multilayers. The multilayers are labeled by the number of atomic layers of [10.1] Co and [110] Cr, respectively. The solid curves are the measured spectra. The dotted curves are the total calculated spectra and, where shown, the dashed curves are the contributions due to only the ML crystallites. The difference between the dotted and dashed curves is due to oriented crystallites of [00.2] Co and/or [110] Cr and [10.1] Co as discussed in the text. The positions corresponding to the various pure orientations in bulk materials are indicated by the dashed vertical lines.

The measured and calculated spectra for several nearly equal layer thickness Co/Cr ML for a variety of bilayer thicknesses are shown in Fig. 2. The labels in the upper right-hand corners correspond to the number of layers of Co and Cr, respectively. The solid curves are measured $\theta-2\theta$ diffraction spectra using Cr $K\alpha$ x rays. The dotted curves are the total calculated intensities for model II and the dashed curves are the calculated contributions to the intensities from only the multilayer crystallites. Note that in the contribution from the ML crystallites of these spectra taken with Cr $K\alpha$ x rays the low-angle satellites always have less intensity than the high-angle satellites. This is due to the variation of the atomic scattering factors of Cr and Co near the $K$ edges and is opposite to the behavior seen in spectra taken with Cu $K\alpha$ x rays. As can be seen the fits are excellent confirming that the multilayers grow in the [110] Cr and [10.1] Co directions with additional crystallites of the pure materials. The positions corresponding to the various orientations for bulk material are indicated by the dashed vertical lines in Fig. 2.

Other orientation combinations in the ML were tried, such as the Co growing initially with the [10.1] orientation followed by some layers in [00.2] direction. These did not fit the measured spectra.

An indication of how much of the total ML film is composed of aligned crystals is given by the height of the background. For layer thicknesses of $<21$ Å the films are essentially composed of only well-oriented multilayers. Above this thickness the fraction of unaligned crystallites grows and becomes appreciable as the layer thickness increases.

One of the most gratifying features of the analysis is that the various parameters are essentially independent of one another. Thus the procedure is to first fit the positions of the main peak and the first upper and lower satellites by adjusting the total number of layers and their effective ratio. Then keeping this ratio as constant as possible the height of the upper satellite is fitted by varying the interface thicknesses. The satellite heights decrease with increasing interface thickness. Since Co and Cr have similar atomic sizes and densities the front and rear interfaces are assumed to have the same thicknesses in Co/Cr ML. This is generally not true for components having appreciably different atomic sizes and structures such as, for example, Mo and Si.[7] The next step is to match the height of the lower satellite and the amount of [10.0] Co by varying the lattice parameters and fractions $f_1$ and $f_2$ of the pure crystallites. The lattice parameters of these small crystallites are often found to be slightly different than the bulk values.

In Table I we list the values for some of the parameters determined by fitting the spectra shown in Fig. 2. As can be seen it is found that for the Co/Cr ML system the average coherence length of nearly equal layer thickness ML crystallites remains fairly constant with a systematic decrease in length from $\sim 200$ Å for small bilayer thickness to $\sim 140$ Å for layer thicknesses of $\sim 50$ Å. The interface thickness is seen to increase with layer thickness. For layer thicknesses $>100$ Å it was found that the spec-

TABLE I. Derived parameters of the Co/Cr multilayer films shown in Fig. 2. All parameters are defined in the text.

| Number of layers Co/Cr | $\Lambda$ (Å) | $L_M$ (Å) | $N_F/N_R$ | $N_1$ | $N_2$ | $f_1,f_2$ | $v_a,v_b$ (%) [00.2]‖[110] | $v_a,v_b$ (%) [10.0] |
|---|---|---|---|---|---|---|---|---|
| 6/7 | 26 | 194 | 6/6 | 25 | 0 | 0.05,0 | 1,16 | 0,0 |
| 11/11 | 44 | 165 | 7/7 | 20 | 0 | 0.12,0 | 4,27 | 0,0 |
| 15.4/14.5 | 59 | 146 | 7/8 | 50 | 12 | 0.10,0.55 | 6,8 | 3,73 |
| 23/21 | 87 | 137 | 11/11 | 70 | 15 | 0.12,1.23 | 9,21 | 2,82 |
| 30/28 | 115 | 143 | 10/10 | 35 | 18 | 0.85,1.00 | 25,16 | 27,58 |

tra can be fit best using only crystallites of the pure materials; that is there is no indication of multilayer formation. This is reasonable since at these thicknesses the coherence length is smaller than the bilayer thickness. For layer thicknesses of $<100$ Å the amount of pure crystallites is seen to increase with layer thickness. It is also seen in Table I that the amount and size of the crystallites of the pure components increases with bilayer thickness. A more complete analysis and discussion of many more series of Co/Cr ML will be given elsewhere.

The assumption that the crystallites have the same length in all directions clearly gives volume fractions ($v_b$) which are unreasonably large for small crystallites. The assumption of equal in-plane areas gives much more reasonable results for the volume fractions ($v_a$). It is thus of great interest to measure the average in-plane dimensions of the crystallites and such work is planned.

It is well known that Co-Cr alloys grow with a columnar structure that could give rise to many of the features seen here. High-resolution transmission electron images of one of the multilayer films have been made[4] and although we could clearly see the layering and columnar structure, with the multilayers growing right through the columns, we could not get good information on the crystallite sizes of the different orientations. More work on this is in progress. It is clear that in order to interpret the measurements of other properties of multilayer films, such as magnetic behavior, ferromagnetic and nuclear magnetic resonance, resistivity, etc., it is necessary to first obtain information about the detailed structure of the films.

## ACKNOWLEDGMENTS

We wish to acknowledge that the ML samples were fabricated by C. H. Lee and the x-ray spectra measurements were made by T. L. Groy. We also thank D. G. Stearns and R. G. Stearns for many discussions and suggestions throughout the course of this work. This work was partially supported by National Science Foundation (NSF) Grant No. DMR-86-10863.

[1]A. Segmuller and A. E. Blakeslee, J. Appl. Cryst. **6**, 19 (1973).

[2]D. B. McWhan, M. Gurvitch, J. M. Rowell, and L. R. Walker, J. Appl. Phys. **54**, 3886 (1983); D. B. McWhan, in *Synthetic Modulated Structures,* edited by L. L. Chang and B. C. Giessen (Academic, New York, 1985), p. 43.

[3]M. B. Stearns, C. H. Lee, and S. P. Vernon, J. Magn. Magn. Mater. **54-57**, 792 (1986).

[4]M. B. Stearns, C. H. Lee, C.-H. Chang, and A. K. Petford-Long, *Metallic Multilayers Systems,* edited by M. Hong, D. V. Gubser, and S. A. Wolf (The Metallurgical Society, Warrendale, PA, 1988), p. 55.

[5]B. E. Warren, *X-ray Diffraction* (Addison-Wesley, Menlo Park, CA, 1969).

[6]W. H. Zachariasen, in *Theory of X-ray Diffraction in Crystals* (Dover, New York, 1945).

[7]A. K. Petford-Long, M. B. Stearns, C.-H. Chang, S. R. Nutt, D. G. Stearns, N. M. Ceglio, and A. M. Hawryluk, J. Appl. Phys. **61**, 1422 (1987).